

Liquid -to-glass transition in bulk glass-forming $\text{Cu}_{55-x}\text{Zr}_{45}\text{Ag}_x$ alloys using molecular dynamic simulations

S SENTURK DALGIC^{1,i} and M.CELTEK²

¹University of Trakya, Science Faculty, Department of Physics, 22030 Edirne-TURKEY

²University of Trakya, Educational Faculty, 22050 Edirne, TURKEY

Abstract. We report results from molecular dynamics (MD) studies concerning the microscopic structure of the ternary, bulk metallic glass-forming $\text{Cu}_{55-x}\text{Zr}_{45}\text{Ag}_x$ ($x=0,10,20$) alloys using tight-binding potentials. Understanding of the nature of Glass Forming Ability (GFA) of studied alloys, GFA parameters, glass transition temperature (T-g), melting temperature (T-m), reduced glass transition temperature (T-g/T-m), the supercooled liquid region and other parameters were simulated and compared with experiments. The computed pair distribution functions reproduce well experimental x-ray data of Inoue and co-workers. Structure analysis of the Cu-Zr-Ag alloy based on MD simulation will be also presented.

1 Introduction

Bulk metallic glasses (BMGs) are promising materials because of their superior properties and relatively lower materials cost. Their low glass-forming ability (GFA) and poor plasticity are points that need further improvement. Recent studies have been interested in order to develop new BMG with improved glass forming ability (GFA). Related to this the Cu-Zr binary alloy system is regarded as a good model system for the investigations on the effect of minor elements added for improvement of both GFA and plasticity [1-7]. Recently, BMG formation in Cu-Zr-Ag alloys has been studied by Inoue, Mattern and co-workers [1-3, 5-7]. The glass forming ability (GFA), crystallization kinetics and structural changes in the family of $\text{Cu}_{55-x}\text{Zr}_{45}\text{Ag}_x$ alloys have also been analyzed by adding Ag to Cu-Zr alloys [1-7]. On the other hand, a few simple criteria were developed in the literature of metallic glass research to explain the GFA of alloys [8-10]. In addition to this, there are less computational approaches proposed to explain the GFA of alloys [8]. According to our knowledge, there are no published simulated structural results for the analysis of GFA ability of the $\text{Cu}_{55-x}\text{Zr}_{45}\text{Ag}_x$ ($x=0, 10, 20$) alloys. There has been only one reported result of Monte Carlo (MC) simulations performed by the modified embedded atom type (MEAM) potentials [11]. It has been shown that, the MEAM potential reproduced the occurrence of the phase separation of Ag rich phases in supercooled Cu-Zr-Ag liquid alloy that is in a good agreement with experimental data [4] and CALPHAD-type thermodynamic calculation [12].

However, recent thermodynamic calculations [13] have predicted the amorphous formation diagram of the Cu-Zr-Ag system based on the available experimental data [4, 5]. Thus the miscibility gap of the liquid phase that was not considered in the calculations of He et al. [12] has been re-optimized by Kang and Jung [13].

In the present work, the GFA ability of ternary $\text{Cu}_{55-x}\text{Zr}_{45}\text{Ag}_x$ ($x=0, 10, 20$) systems are firstly evaluated by molecular dynamics (MD) calculations in which the atomic interactions are modeled with a many body type potential as tight binding (TB) potential (called as n-body Gupta potential) proposed by Cleri and Rosato [14]. In order to investigate the liquid to glass transition in Cu-Zr-Ag BMGs on an atomic level, TB potentials for the pure Cu, Zr and Ag has been used to newly developed for the ternary Cu-Zr-Ag system. This potential yields the liquid to glass transition in the ternary $\text{Cu}_{55-x}\text{Zr}_{45}\text{Ag}_x$ ($x=0, 10, 20$) alloys, in a good agreement with recent calculations of Kang and Jung [13].and also experimental data [4].

2 Method

As a first step in MD simulations, it is necessary to describe the atomic motions. In this study we have used a quantum mechanics based TB potential [12] to describe the atomic motions and to explain the structural properties. In TB approach, the total potential energy of a system is given the following form :

$$E = \sum_i \left[A_{ij} \sum_{j \neq i} \exp \left[-p_{ij} \left(\frac{r_{ij}}{r_{0ij}} - 1 \right) \right] - \left(\sum_{j \neq i}^2 [-2q_{ij} \left(\frac{r_{ij}}{r_{0ij}} - 1 \right)] \right)^{1/2} \right] \quad (1)$$

where r_{ij} represents the distance between atoms i and j ; r_0 is the interatomic distance between the nearest neighbours, A , ξ , p and q are parameters fitted to the experimental values of the bulk cohesive energy, lattice parameters and elastic constants. In order to describe the pair interaction between different types of atoms, the following combination rules are utilized.

$$A_{ij} = \sqrt{A_i A_j}, \quad \xi_{ij} = \sqrt{\xi_i \xi_j} \quad (2)$$

$$q_{ij} = \frac{q_i + q_j}{2}, \quad p_{ij} = \frac{p_i + p_j}{2}, \quad r_{0ij} = \frac{r_{0i} + r_{0j}}{2} \quad (3)$$

To describe an alloy system, the pair interaction between different elements should be determined. For this, a similar technique that is used to determine the pair interaction for pure elements is applied to binary alloy systems.

In our simulations, we have used the simulation code of DL_POLY [15]. The Finnis-Sinclair type metal potential of Gupta potential as the same form as TB potential embedded in DL_POLY code is used. MD simulations are performed in a cubic box subject to periodical boundary conditions for a system with 2000 particles under zero external pressure. The NPT ensemble with the Berendsen thermostat has been used to control the temperature and pressure. The MD simulations have been started from a super cell box with 2000 atoms and created for the compositions $\text{Cu}_{55}\text{Zr}_{45}$, $\text{Cu}_{45}\text{Zr}_{45}\text{Ag}_{10}$ and $\text{Cu}_{35}\text{Zr}_{45}\text{Ag}_{20}$ with periodic boundary conditions. To generate the exact compositions, we randomly changed 100 Cu atoms by the same number of Zr atoms (starting from the B2 structure of $\text{Cu}_{50}\text{Zr}_{50}$ (Cu_1Zr_1) with 2000 atoms) for $\text{Cu}_{55}\text{Zr}_{45}$, for $\text{Cu}_{45}\text{Zr}_{45}\text{Ag}_{10}$ alloy 200 Ag atoms changed by 100 Cu and 100 Zr atoms, also for $\text{Cu}_{35}\text{Zr}_{45}\text{Ag}_{20}$ alloy case the same procedure is used. Verlet leapfrog algorithm with a time step 2 fs has been used for the integration of the Newtonian equations.

The stable structure at 0 K is obtained through the initial configurations annealed fully at $T=300$ K and then cooled to $T=0$ K at a cooling rate of 0.25 K/ps. A series temperature increases from 0 K to 1800 K with an increment of 50 K are carried out at the heating rate 0.5 K/ps. The final temperature of 1800 K is a few hundred degrees above the melting point to avoid the overheating of the system. Before starting the cooling process, the system in liquid state is equilibrated at 1800 K using (NVT) ensemble with 300000 steps. Then, the system is cooled with different cooling rates from 1800 K to 300 K.

3 Results and discussions

The MD simulations using the DL_POLY simulation code [15] have been performed with TB form of Gupta potentials at the different heating and cooling rates. The input potential parameters for Cu, Ag, and Zr are listed in Table 1.

Figure 1. shows the temperature dependence of the volume of $\text{Cu}_{55-x}\text{Zr}_{45}\text{Ag}_x$ ($x=0, 10, 20$) alloys during the heating and cooling process.

Table 1. TB potential parameters for Cu, Ag and Zr

metal	A(eV)	ξ (eV)	p	q	r_0 (Å)
Cu	0.0855	1.2240	10.960	2.278	2.56
Ag	0.1028	1.1780	10.928	3.139	2.89
Zr	0.1934	2.2792	8.2500	2.249	3.17

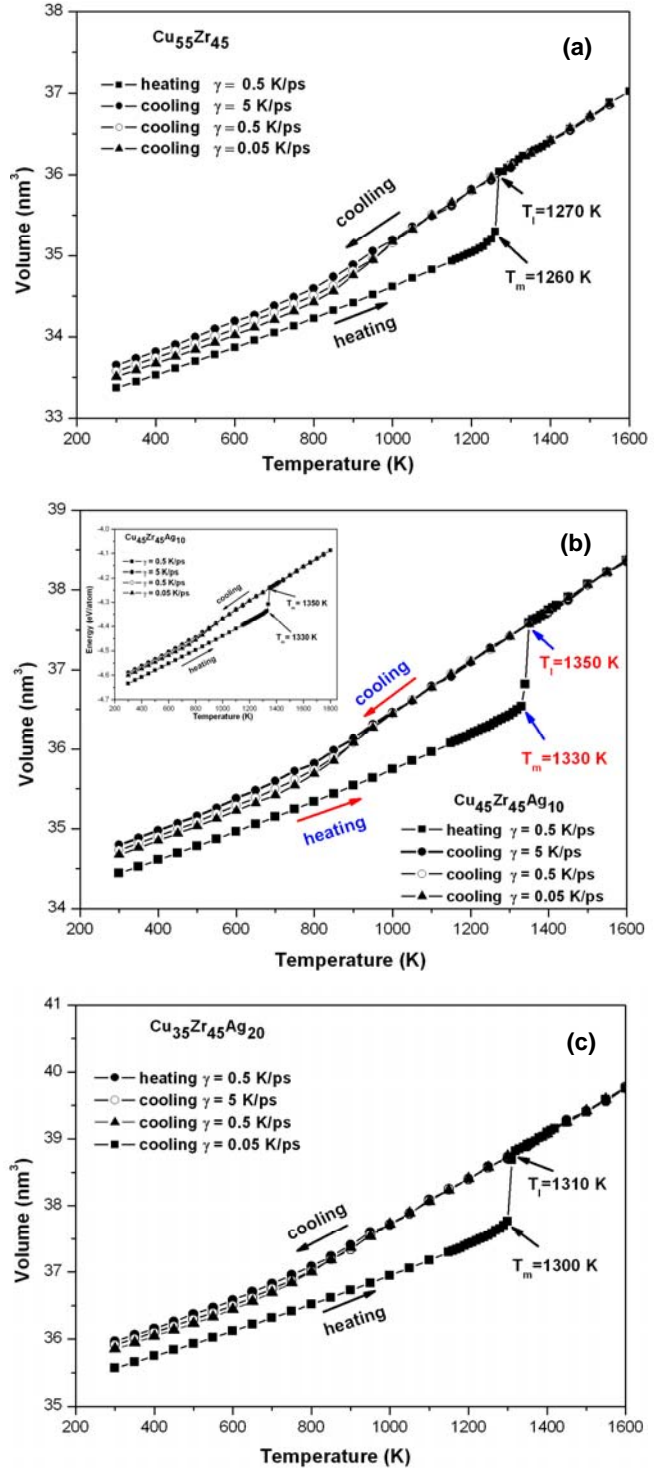


Fig. 1. The temperature dependence of volume of $\text{Cu}_{55-x}\text{Zr}_{45}\text{Ag}_x$ ($x=0, 10, 20$) alloys at heating and cooling process.

As shown in Fig.1, the heating curves bends upward as the melting (melting temperature T_m), and overlaps the cooling curves upon complete melting (the liquidus temperature T_l). To ensure complete melting an ultimate temperature of 1800 K was reached. We have also illustrated the temperature dependence of cohesive energy of $\text{Cu}_{35}\text{Zr}_{45}\text{Ag}_{20}$ in Fig. 1b. Figure 2 shows the simulated pair distribution functions (PDF) at different temperatures during the heating and cooling process

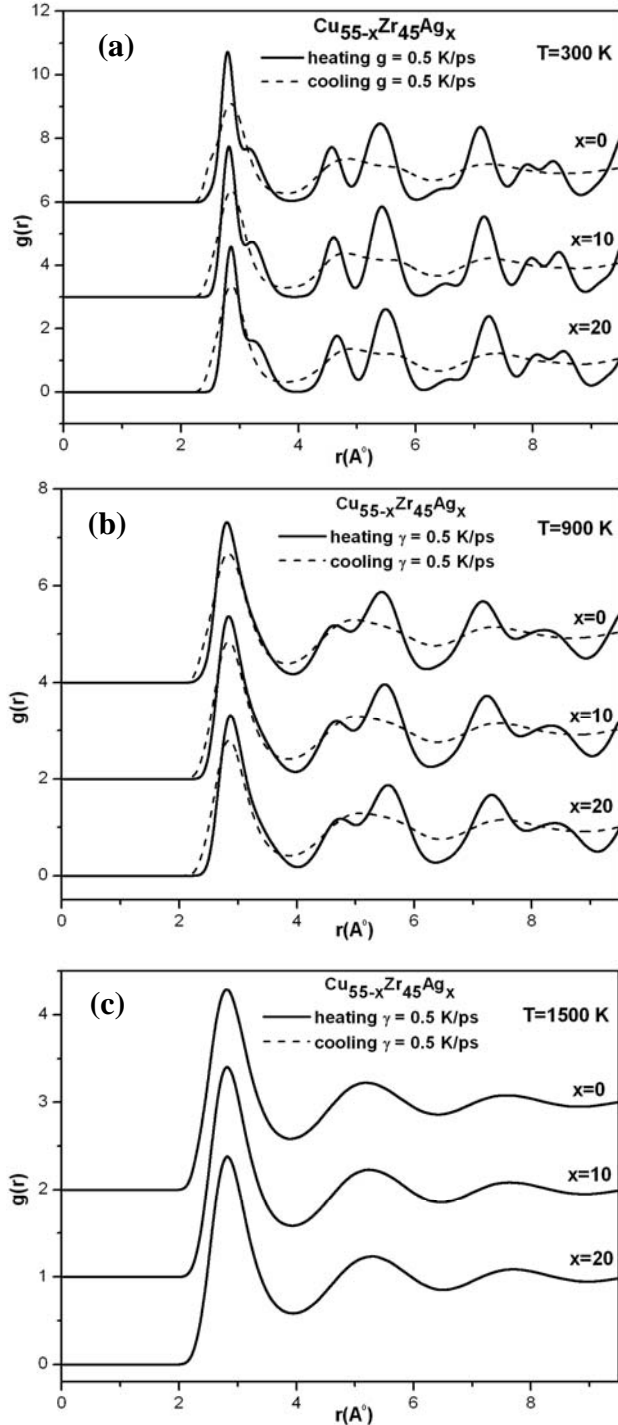


Fig. 2. The total pair distribution functions (PDF) of $\text{Cu}_{55-x}\text{Zr}_{45}\text{Ag}_x$ ($x=0, 10, 20$) alloys in heating and cooling process.

There are several methods for determining the melting temperature of a crystal. The point where the volume (or cohesive energy) shows discontinuity is taken as the melting point. The calculated melting temperatures of presented alloys under zero pressure are listed in Table2. In Figs.1, the change of the volume exhibits only subtle changes at the glass transition temperature. There is no dramatic drop observed in the mean atomic energy upon the whole cooling. However, we do see a change in the PDF. Thus the glass transition temperature T_g for the $\text{Cu}_{55-x}\text{Zr}_{45}\text{Ag}_x$ ($x=0, 10, 20$) ternary alloys is defined by the temperature at the intersection of the extrapolations of the liquid and glassy plots..

Fig. 2, exhibits the changes of the total simulated PDF for all presented alloys during heating and cooling process. As shown in Fig. 2(a), at the temperature of 300K in heating process, the whole system is in a crystalline state and the PDF curve is similar as the bcc crystal. While the total PDF shows a split in the second peak for the all presented metallic glasses at the same temperature during cooling process, it is a typical feature of glass formation, showing that quenching the $\text{Cu}_{55-x}\text{Zr}_{45}\text{Ag}_x$ ($x=0, 10, 20$) alloys from liquid to 300K at the cooling rate of 0.5K/ps leads to the metallic glass. This split is indicative of amorphous atomic packing. Whether in heating or cooling process, at the temperature of 1500K, the systems are in an equilibrium liquid state as shown in Fig. 2(c).

We also determined the GFA parameters of the $\text{Cu}_{55-x}\text{Zr}_{45}\text{Ag}_x$ ($x=0, 10, 20$) ternary alloys deduced from MD simulations. The simulated GFA parameters are listed in Table 2. The parameter of $T_{rg}^* = T_g/T_l$ is calculated while the liquidus temperature T_l is taken as equal to T_m the melting point of presented alloys ($T_l=T_m$)

We have also considered different cooling rates to investigate its effect on the glass transition temperature T_g . A parameter often used to define the glass transition temperature is the Wendt-Abraham (WA) parameter which is defined by $R^{WA} = g_{\min} / g_{\max}$, where g_{\min} and g_{\max} denote the first minimum and first maximum of the PDF. Fig. 3 shows the temperature dependence of the WA parameters of the simulated $\text{Cu}_{35}\text{Zr}_{45}\text{Ag}_{20}$ ternary alloy, at three different cooling rates.

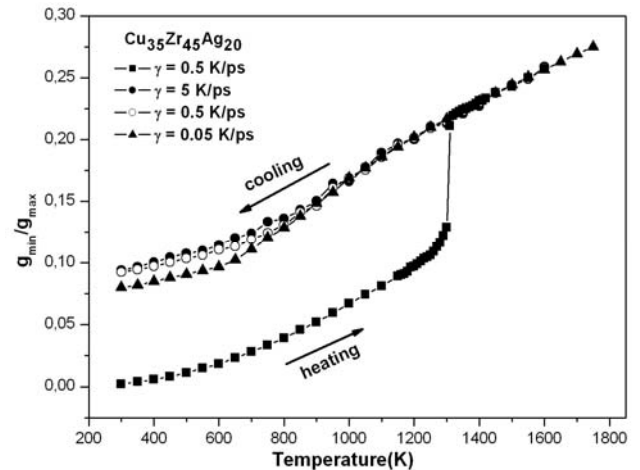


Fig. 3. WA parameters as a function of temperature in $\text{Cu}_{35}\text{Zr}_{45}\text{Ag}_{20}$ ternary alloy.

Table 2. The GFA parameters of $\text{Cu}_{55-x}\text{Zr}_{45}\text{Ag}_x$ ($x=0, 10, 20$) alloys obtained from a heating rate of 0.5 K/ps and different cooling rates.

Composition	T_m^{MD} (K)	γ^{MD} (K/ps)	T_g (K)		T_{rg}^* T_g^*/T_1	T_1 (K)		T_{rg} (T_g/T_1)	
			MD	Exp.		MD	Exp.	MD	Exp.
$\text{Cu}_{55}\text{Zr}_{45}$	1260±10	5	760	682 ^a	0.603	1137 ^a	0.598	0.600 ^a	
		0.5	710	694 ^b	0.564	1270±10	1183 ^{b,f}	0.559	0.587 ^f
		0.05	670		0.532			0.528	
$\text{Cu}_{45}\text{Zr}_{45}\text{Ag}_{10}$	1330±10	5	712	683 ^c	0.535		1142 ^c	0.527	0.598 ^c
		0.5	680	684 ^d	0.511	1350±10	1140 ^{d,f}	0.504	0.600 ^d
		0.05	645		0.485			0.478	0.596 ^{e,f}
$\text{Cu}_{35}\text{Zr}_{45}\text{Ag}_{20}$	1300±10	5	710	680 ^e	0.546			0.542	
		0.5	683	677 ^f	0.525	1310±10	1203 ^f	0.521	0.563 ^f
		0.05	595		0.458			0.454	

^aRef [7], ^bRef [16] ^cRef [2], ^dRef [1], ^eRef [4], ^fRef [6], ^gRef [17]

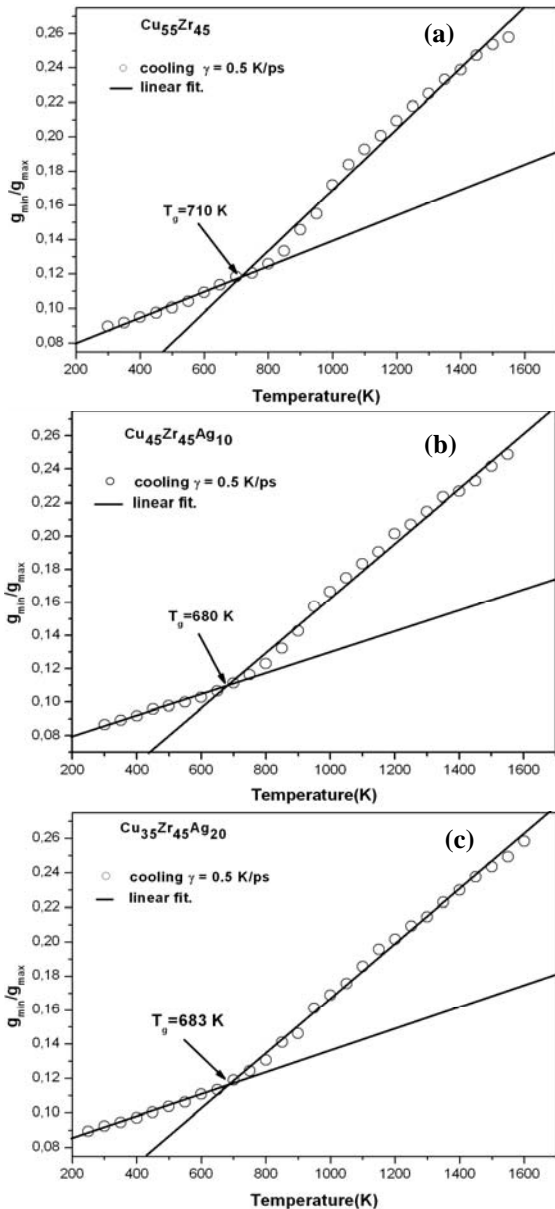


Fig. 4. Temperature dependence of $g_{\text{min}}/g_{\text{max}}$ values fitted to a linear function to estimate the glass temperature T_g

In Figure 4, it has been illustrated the values of $g_{\text{min}}/g_{\text{max}}$ fitted to a linear function to estimate the glass temperature T_g at the cooling rate of $\gamma=0.5\text{K/ps}$.

As shown in fig. 3 and fig. 4, each cooling rate leads to a slightly different value of for the temperature at which the slope changes. The remaining low temperature and high temperature data sets are fitted to linear.

The total PDF of $\text{Cu}_{55-x}\text{Zr}_{45}\text{Ag}_x$ ($x=0, 10, 20$) alloys have been calculated at 720 K on the basis of this model. The simulated results of total PDF are presented in Fig. 5 along with the experimental x-ray data of Inoue and co-workers [3, 6].

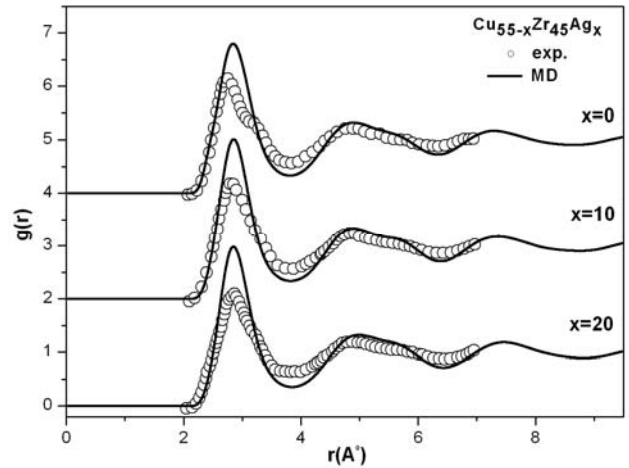


Fig. 5. The simulated total PDF of $\text{Cu}_{55-x}\text{Zr}_{45}\text{Ag}_x$ ($x=0,10,20$) alloys at 720 K along with experimental data of Inoue [3, 6]

As shown in Fig. 5, there is a good agreement between our simulation results and experiment.

4 Conclusion

The present contribution reports results from a MD modeling of the ternary $\text{Cu}_{55-x}\text{Zr}_{45}\text{Ag}_x$ ($x=10, 20$) alloys.

Up to date no works dedicated the GFA or BMG forming of the Cu-Zr-Ag ternary system by MD simulations with TB potentials.

The presented $\text{Cu}_{55-x}\text{Zr}_{45}\text{Ag}_x$ ($x=0, 10, 20$) alloys also show a typical feature of glass formation, that quenching from liquid to 300K at the cooling rate of 0.5K/ps leads to the metallic glasses. As known that splitting of the first maximum in the total PDF indicates the lower GFA. The experimental and simulated data are in good agreement for $\text{Cu}_{55-x}\text{Zr}_{45}\text{Ag}_x$ ($x=10, 20$) alloys

MD results are agree well with the Inoue's empirical rule [10] for the increasing of T_g at the cooling rates of 5 and 0.5K/ps. The simulated glass transition temperature T_g of $\text{Cu}_{45}\text{Zr}_{45}\text{Ag}_{10}$ ternary alloy is about 680K at the cooling rate of 0.5K/ps that is 4K lower than the reported experimental value given in Ref [1].

For the MD simulations in the cooling rates of 5 and 0.5K/ps the T_g values of the ternary alloys remains almost unchanged with increasing Ag content to $\text{Cu}_{55}\text{Zr}_{45}$ binary alloy, as indicated experimentally in Ref.[7]. The MD results are agree well with experimental and thermodynamic data [6,13]. It has been shown experimentally that Ag content significantly affects the liquidus temperature T_l and melting behaviour of these alloys. The lowest T_l and highest T_g/T_l was observed for $\text{Cu}_{45}\text{Zr}_{45}\text{Ag}_{10}$ alloy case while the MD simulations predict that the highest value of T_{rg} is achieved for $\text{Cu}_{55}\text{Zr}_{45}$ alloy.

According to the recent thermodynamic data given in Ref. [13], the presented compositions of $\text{Cu}_{55-x}\text{Zr}_{45}\text{Ag}_x$ ($x=0, 10, 20$) alloys have been shown as fully amorphous state that is in good agreement with our MD results.

References

1. W. Zhang, A. Inoue, J. Mater. Res. **21**, 234 (2006).
2. W. Zhang, F. Jia, Q. Zhang, A. Inoue, Mater. Sci. Eng. A **459**, 330 (2007).
3. D. V. Louzguine-Luzgin, K. Georgarakis, A. R. Yavari, G. Vaughan, G. Xie, A. Inoue, J. Mater. Res. **24**, 274 (2009)
4. A. A. Kündig, M. Ohnuma, T. Ohkubo, T. Abe, K. Hono, Scripta Mater. **55**, 449 (2006).
5. D. V. Louzguine-Luzgin, G. Xie, W. Zhang, A. Inoue, Mater. Sci. and Eng. A, **465**, 146 (2007), *ibid*: Mater. Sci. and Eng. A **527**, 2146 (2010).
6. D. V. Louzguine-Luzgin, G. Xie, W. Zhang, T. Saito, K. Georgarakis, A. R. Yavari, G. Vaughan, A. Inoue, Journal of Phys.: Conf. Series **144**, 012047 (2009).
7. N. Mattern, A. Schöps, U. Kühn, J. Acker, O. Khvostikova, J. Eckert, J. Non-Cryst. Solids **354**, 1054 (2008).
8. C. H. Lee, T. Cagin, W. L. Johnson, W.A. Goddard, J. Chem. Phys. **119**, 9858 (2003).
9. C. Suryanarayana, I. Seki, A. Inoue, J. Non-Cryst. Solids **355**, 355 (2009).
10. A. Inoue, Acta Mater. **48**, 279 (2000)
11. K.-H. Kang, I. Sa, J. -C. Lee, E. Fleury, B. J. Lee, Scripta, Mater. **61**, 801 (2009).
12. X. C. He, H. Wang, H. S. Liu, Z. P. Jin, CALPHAD **30**, 367 (2006).
13. D. H. Kang, I-H Jung, Intermetallics, **18**, 815 (2010).
14. F. Cleri, V. Rosato Phys. Rev. B **48**, 22 (1993).
15. DL_POLY: a molecular dynamics simulation package written by W. Smith, T.R. Forester and I.T. Todorov has been obtained from the website http://www.ccp5.ac.uk/DL_POLY
16. W. F. Gale, T.C. Totemeier (Eds.), *Smithells, Metals Reference Book, 8th ed.*, Elsevier, Burlington, pp. 11 (2004).
17. D. Nagahama, T. Ohkubo, T. Mukai, K. Hono, Mater. Trans. **46**, 1264 (2005).

ⁱ *Corresponding author: S. Senturk Dalgic, e-mail: serapd@trakya.edu.tr